Gramicidin-S-Inspired Cyclopeptidomimetics as Potent Membrane-Active Bactericidal Agents with Therapeutic Potential

Chengfei Hu, Quan Wen, Shuhui Huang, Saisai Xie, Yuanying Fang, Yi Jin, Rémy Campagne, Valérie Alezra, Emeric Miclet, Jinhua Zhu, et al.

Gramicidin S-inspired Cyclopeptidomimetics as Potent Membrane-active Bactericidal Agents with Therapeutic Potential

Chengfei Hu,[‡[a]] Quan Wen,[‡[a]] Shuhui Huang,[[b]] Saisai Xie,[[a]] Yuanying Fang,[[a]] Yi Jin,[[a]] Rémy Campagne,[[c]] Valérie Alezra,[[c]] Emeric Miclet,[[d]] Jinhua Zhu,[[e]]* Yang Wan [[a][c]]*

[a] National Pharmaceutical Engineering Center for Solid Preparation in Chinese Herbal Medicine, Jiangxi University of Traditional Chinese Medicine, 1688 Meiling Avenue, WanLi, Nanchang 330004, P. R. China

E-mail: wy15506@gmail.com

[b] Jiangxi Maternal and Child Hospital, Nanchang 330006, P. R. China

[c] Laboratoire de Méthodologie, Synthèse et Molécules Thérapeutiques (ICMMO), Université Paris-Sud, UMR 8182, CNRS, Université Paris-Saclay, Bât 410, Facultédes Sciences d'Orsay, Orsay, 291405, France

[d] Sorbonne Université, École normale supérieure, PSL University, CNRS, Laboratoire des biomolécules, LBM, 75005 Paris, France

[e] Institute of Traditional Chinese Medicine, Jiangxi University of Traditional Chinese Medicine, 1688 Meiling Avenue, WanLi, Nanchang 330004, P. R. China

‡ These authors contributed equally to this work.

Abstract: Antimicrobial peptides (AMPs) are promising antibacterial agents often hindered by their undesired hemolytic activity. Inspired by gramicidin S (GS), a well-known cyclodecapeptide, we synthesized a panel of antibacterial cyclopeptidomimetics using β,γ-diamino acids (β,γ-DiAAs). We observed that peptidomimetic CP-2 displays a bactericidal activity similar to that of GS while possessing lower side-effects. Moreover, extensive studies revealed that CP-2 likely kills bacteria through membrane disruption. Altogether, CP-2 is a promising membrane-active antibiotic with therapeutic potential.

Introduction

Since their discovery at the beginning of the 20th century, Penicillin, Sulfonamide and their subsequent chemical derivatives have been used as the first-line antibiotics to combat microbial infections for several decades and are still widely used today.[1] Both Penicillin and Sulfonamide are metabolic antagonists of bacteria-specific physiological processes: cell wall and folate biosynthesis, respectively. This antibacterial strategy of targeting bacteria-specific processes has deeply influenced the development of antibiotics in the following decades.[1] Since these processes are absent from human cells, these antibiotics usually exert highly selective toxicity towards bacterial cells. However, they also provide opportunities for bacteria to become resistant. As a consequence, multidrug-resistance (MDR), extensive drug-resistance (XDR) and pandrug-resistance (PDR) of bacteria today have become a major issue for human healthcare.[2,3] Therefore, antibiotics with new mechanisms of action are urgently needed to combat the ever growing health threat posed by resistant pathogenic microorganisms.[4]

Antimicrobial peptides (AMPs) are a category of naturally occurring molecules that display an extraordinarily broad range of antimicrobial activities covering both Gram-positive and Gram-negative bacteria.[5] Although originating from a large variety of organisms, they are usually classified into α-helical or β-sheeted groups with cationic, hydrophobic and amphiphilic characteristics.[6] To date, near 3000 AMPs have been characterized and biologically evaluated.[6] There is wide acceptance that AMPs kill microorganism mainly through the disruption of lipid bilayers of their cell membrane.[7] Such model of action is significant as it can minimize bacterial resistance possibilities since there are no specific membrane targets. This is why there is no essential resistance observed against ancient AMPs like gramicidin S (GS) and tyrocidines that have been clinically used for more than seventy years and are still used today.[8] In this regard, AMPs are appealing targets for the development of novel antibiotics.[5] Unfortunately, these membrane-active peptides are rather indiscriminate between bacterial and human cells, leading to an undesired hemolytic effect.[9] As a result, the majority of clinical applicable AMPs are used or designed for topical applications only with very

few exceptions aimed for systematic applications.[5] To overcome these limitations, many different strategies, including but not limited to structural/sequence modification,[10–13] specific delivery system design,[14–17] "smart" AMPs[18–20] and *de novo* designed antimicrobial peptides/peptidomimetics[21–27] have been developed to efficiently use AMPs without being hindered by their side-effects. Among these strategies, modification or mimicry of naturally occurring peptides with natural amino acids or unnatural building blocks is an efficient pathway.[10,21,28]

The aforementioned gramicidin S (GS), a well-known AMP obtained from bacteria, is active against a wide range of Gram-positive and Gram-negative bacteria, as well as viruses, fungi and tumors.[10,29–31] Structurally, it is a cyclodecapeptide with the primary sequence *cyclo*-(VOL^{D}FP)$_2$ (where O stands for ornithine), which adopts a rigid C_2-symmetric β-hairpin structure (**Figure 1**, left panel). The global conformation is constrained by four intra-molecular H-bonds with four hydrophobic side-chains (Val and Leu) positioned on the opposite face from the two Orn cationic side chains, resulting in a strong amphiphilicity.[32,33] To lower its hemolytic effect, which severely hampers its therapeutic potential, GS structure has been extensively optimized or mimicked by different approaches to reach non-toxic GS-based antibiotics.[10,13,28,34–37] However, to date, there is no systematically applicable antibiotic based on GS available and thus a constant investment in this field is needed. Our group is strongly involved in the synthesis of β,γ-diamino acids (β,γ-DiAAs) as well as their incorporation in peptide chains.[38–41] We have reported several studies which established the possible involvement of the supplemental amino groups in extra hydrogen bonds.[39,40] More recently, we have demonstrated that the replacement of ^{D}Phe-Pro in the β-turn region by turn mimics β,γ-diamino acids (β,γ-DiAAs) affords GS analogues endowed with retained activity but no hemolytic effect.[42,43] In this work, four aromatic β,γ-DiAAs differing in stereochemistry were used to reinforce the amphiphilic character of GS-inspired cyclopeptidomimetics (**Figure 1**, left panel). We showed that peptidomimetic **CP-2** is as toxic as GS towards bacterial cells while being relatively less toxic to human cells. Bactericidal mechanism studies revealed that **CP-2** likely kills bacteria by disrupting their membrane.

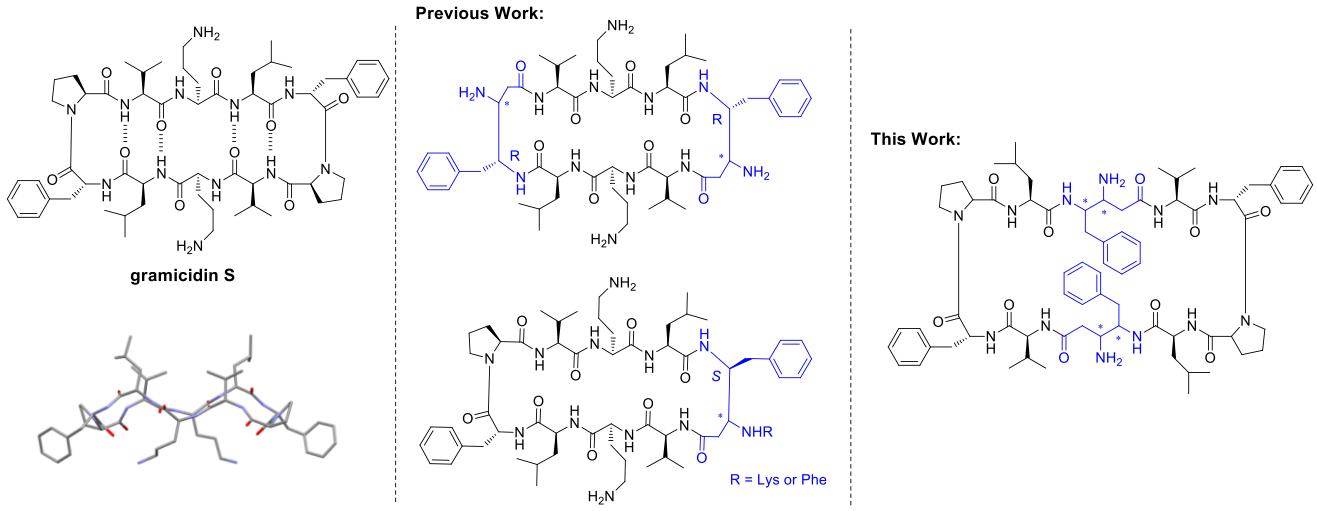

Figure 1. Structure of gramicidin S (GS) and side view of its X-ray crystallographic structure (left panel). Structures of previously reported GS-based cyclopeptidomimetics[42,43] (middle panel) and GS-inspired cyclopeptidomimetics of this work (right panel).

Results and Discussion

Peptide Design and Synthesis

Peptide Design. Recently, one of our studies showed that β,γ-DiAAs are capable of promoting dimerization when incorporated into α/γ-hybrid tripeptides through extra hydrogen bonds.[44] We thereby questioned whether these short peptides could serve as β-strand mimics in cyclopeptides. Inspired by the GS sequence, we employed hydrophobic residues (Xxx = Val or Leu) and the β-turn inducer '^{D}Phe-Pro' to constrain the dimeric tripeptide at both ends (**Figure 2**). We chose β,γ-DiAAs derived from the phenylalanine as it provides additional hydrophobicity (phenyl group), while bearing the NH_2 group which is found on the ornithine side chain of the GS sequence. Such an aliphatic character is of prime importance to maintain the biological activity of GS analogues.[35,37,43]

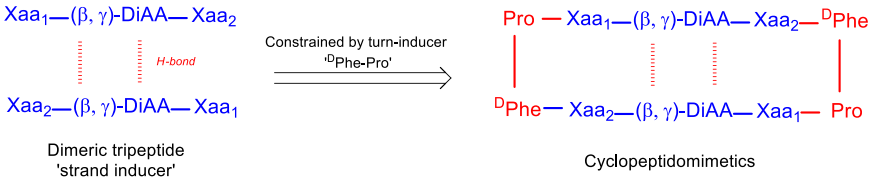

Figure 2. Design of cyclopeptidomimetics. **Xaa**: Val or Leu

Peptide Synthesis. The synthesis of β,γ-DiAAs was achieved according to previously reported procedures.[42,43,45] All other α-amino acids are commercially available. The synthesis of cyclopeptidomimetics begins by building the linear sequence on solid phase starting from Fmoc-Pro-2-Chlorotrityl Chloride (CTC)-Resin. Linear peptidomimetics were cleaved from resin by 1% TFA/DCM (v/v) to keep side-chain protections intact. Macrocyclization was carried out in highly diluted solution to minimize undesired heterodimerization. After global deprotection in 90% TFA/water (v/v), crude peptides were purified by reverse-phase high performance liquid chromatography (RP-HPLC). Four distinct cyclopeptidomimetics based on β,γ-DiAAs were synthesized (**Scheme 1**) and characterized by high resolution mass spectrometry (HRMS).

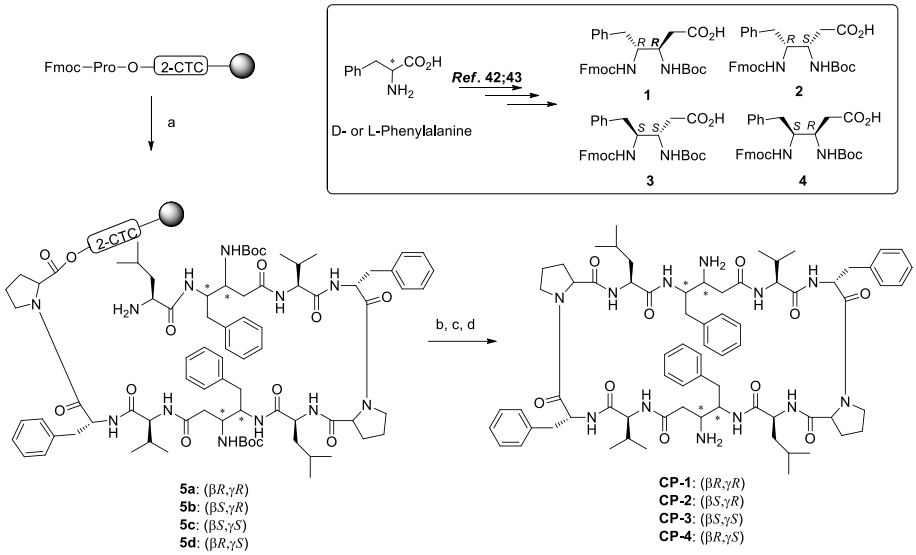

Scheme 1. Synthesis of cyclopeptidomimetics. (a) Sequential coupling (Xaa or β,γ-DiAA, HBTU, DiPEA, DMF) and deprotection (20% piperidine/DMF, v/v) steps; (b) 1% TFA/DCM, v/v, 5x 10 min; (c) PyBOP, HOBt, DiPEA, DMF; (d) 90% TFA/water, v/v. Inset: synthesis of β,γ-DiAAs.

Biological Activities

Minimal Inhibitory Concentration (MIC) Determination. To evaluate the biological activities of the synthetic cyclopeptidomimetics, we started with the determination of MIC values using a series of bacteria covering both Gram-negative and Gram-positive strains. GS was used as a reference. As expected, GS displays high bactericidal activity towards Gram-positive strains while being less active against Gram-negative strains.[10] Similarly to GS, all cyclopeptidomimetic show no obvious activity against Gram-negative strains. However, they have different antibacterial activities against Gram-positive ones, despite sharing a similar chemical skeleton. In general, **CP-2** shows the best antibacterial activity, comparable to that of GS (**Table 1**). Peptide **CP-1** is less active whereas **CP-3** and **CP-4** are almost totally inactive. Interestingly, these biological activities appears to be linked to the structural properties of the four analogues, **CP-2** displaying the more intense CD spectra (**Figure 5**). .

Table 1. Antibacterial activity of synthetic cyclopeptidomimetics and GS[a][b]

Peptide	RP-HPLC Retention Time (min)	Gram-negative bacteria		Gram-positive bacteria				
		E. coli	*P. aeruginosa*	*S. aureus*	*B. subtilis*	*S. bovis*	*E. faecalis*	*E. faecium*
GS	48.5	50	50	3.13	3.13	6.25	6.25	3.13
CP-1	37.5	>100	>100	25	50	25	12.5	25
CP-2	33.8	>100	>100	6.25	12.5	12.5	6.25	12.5
CP-3	35.2	>100	>100	50	50	25	50	25
CP-4	34.6	>100	>100	>100	50	50	>100	50

[a] measured as MIC (μg/mL). [b] 100 μg/mL was the maximal tested concentration.

Hemolytic Activity. We next evaluated the hemolytic activity of the synthetic peptidomimetics in comparison to GS. It is widely known that GS induces hemolysis at a very low concentration.[29] Notably, none of our synthetic peptidomimetics lyzes human red blood cells as much as that GS does (**Figure 3**). There is a general trend that the higher antibacterial activity is associated with stronger hemolysis. Although **CP-2** exerts the most pronounced hemolysis among the synthetic peptidomimetics, the concentration required for 100% hemolysis (approximately 250 μg/mL) is much higher than that of GS (approximately 70 μg/mL), leading to a better therapeutic index. As an empirical method, the amphiphilicity of peptides were estimated using the RP-HPLC retention times. As shown in **Table 1**, all cyclopeptidomimetics have rentention times short than GS. Since hemolytic activity is highly associated with amphiphilicity of AMPs,[34] it contributes to explain why peptidomimetics exhibited lower hemolysis than GS.

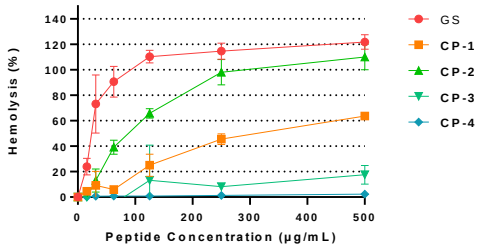

Figure 3. Hemolytic activity of the synthetic cyclopeptidomimetics and GS. Percentage hemolysis, mean ± value, and $n = 3$. The reference for 100% hydrolysis has been measured using 0.1% w/v SDS solutions (see Experimental section).

Cytotoxicity. To further examine the biocompatibility, we evaluated the cytotoxicity of the synthetic peptidomimetics using human normal liver cells LO2. Cytotoxicity was determined by measuring the cell viability. Cell Counting Kit-8 (CCK-8) assays were carried out in cell medium supplemented with 1% fetal bovine serum. As can be been seen in **Figure 4**, GS starts to show toxicity at a concentration of 5 μg/mL, a point where no toxicity is observed for any synthetic peptidomimetic. For the most active peptidomimetic **CP-2**, a significant cytotoxicity is only observed at concentrations higher than 10 μg/mL.

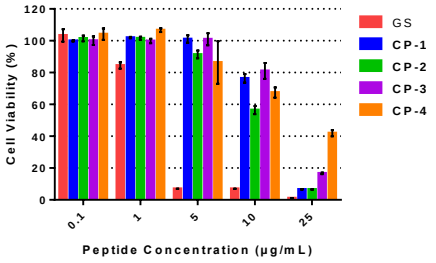

Figure 4. Cytotoxicity of the synthetic cyclopeptidomimetics and GS. Percentage cell viability, mean ± value, and $n = 3$.

Structure-activity Relationship (SAR) Studies

Circular Dichroism (CD) Spectroscopy Studies. To evaluate their secondary structure, CD spectra of peptidomimetics and GS were measured in various solution (**Figure 5**). As it is known, GS adopts stable β-hairpin struture. The simultaneous presence of β-sheet and β-turn are characterized by the two negative shoulders around 207 and 220 nm.[34] The CD spectra of GS becomes more intense when placed in MeOH (hydrophobic environment), suggesting a stabilization of its structure. In TFE/water, the GS spectrum corresponds to an averaged CD signal between the spectra recorded in water and in MeOH, which suggests an intermediate structure between these two close conformations. In SDS micelles, the CD spectrum of GS is very similar to the one observed in water, although the band at 220 nm is less intense, as observed in hydrophobic environments. This may results from the interaction of GS with the micelle surface. As far as **CP**-2 is concerned, its CD spectra is characterized by a minimum at 196 nm, much more pronounced in hydrophobic environment or in SDS micelles which demonstrate the CP-2 interacts with the hydrophobic core of the micelles. A large negative band is also observed between 200 and 240 nm, which differs from random coil spectra where almost no signal is found between 210 and 240 nm. Interestingly, this large band is amplified in the TFE/water and the difference spectra obtained between TFE/water and water are very similar between **CP**-2 and GS (**Figure 5E**). No precise structural information can be deduced from this observation but it may reveal a common conformational change from water to hydrophobic environments. **CP**-3 and **CP**-4 are poorly structured both in water and in MeOH (and consequently, also in the TFE/water mixed solvent). In the presence of micelles, they undergo a folding that recalls the β-sheet structure of GS in water. As the spectrum in MeOH is very weak in methanol for these two peptides, it is unlikely that they are located inside the micelles but they probably interact with the micelle surface which stabilizes a β-sheet structure. Finally, CP-1 displays the same weak spectra in water, MeOH, and in SDS micelles which suggests a highly dynamic structure with no influence of the solvent. Thus, **CP**-2 is the only GS analog which has a structure affected both by the hydrophobic environment and the presence of micelles. This is a strong indication that **CP**-2 can interact with the hydrophobic core of the SDS micelles. This specific location is compatible with a pore formation that can disrupt the bacterial membrane. Interestingly, the CD spectrum of CP-2 in water is reminiscent of the spectrum obtained previously on a cyclic decapeptide GS analogue,[34,46] which retained interesting antibacterial activity.

Thus, there is no direct correlation between the stability of the β-hairpin structure and the biological activity of the GS analogues. It is interesting to note that CP3 and CP4 both display a β-hairpin struture in micelles although they possess the poorest antibacterial activities. These two analogues share a (*S*) configuration at the DiAA Cγ. Hence the aromatic side chains point toward the same half-plane than the phenyl groups of the ^{D}F. This four side chains may form an aromatic patch that interacts with the membrane models and stabilize the β-hairpin conformation. However in GS structure, the hydrophobic face is composed by the aliphatic residues V, L and P, that are located on the other side. Without the long polar chain of the O residue found in the native sequence of GS, CP3 and CP4 could be flipped on the membrane surface compared to GS. With a (*R*) configuration at the Cγ of the DiAAs, the aromatic side chains of CP1 and CP2 could reinforce the hydrophobic character created by the V, L and P residues, although the native β-hairpin struture of GS is not conserved for these peptides. CP1 was unstructured in all the solvent tested, whereas CP2 adopted a non canonical structure, stabilized in methanol, TFE/water and in SDS micelles. The Cβ of the DiAAs bears the polar amonium group and its configuration play a important role for both the structure and the activity oft he GS analogues. Thiese results highlight the relevance of using chiral DiAAs for the design of new GS analogues.

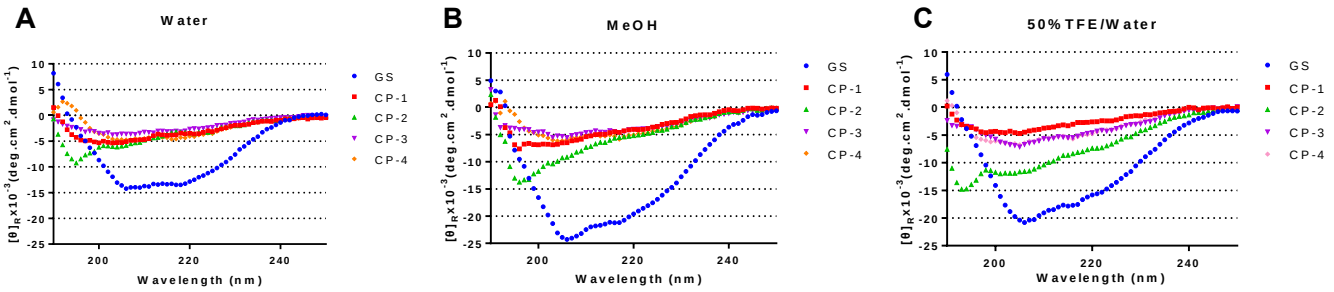

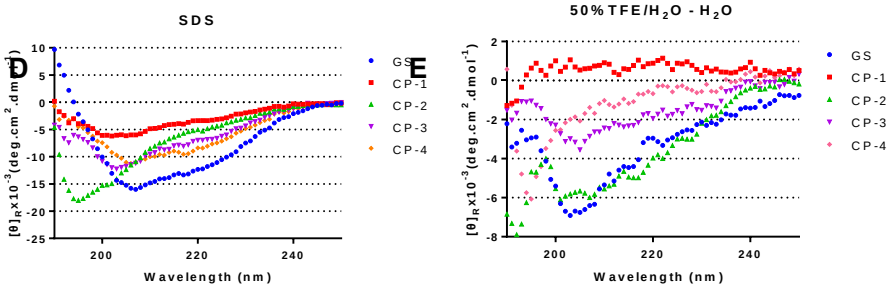

Figure 5. CD spectra of synthetic cyclopeptidomimetics (0.1 mM) in various solution.

Antibacterial Mechanism

Time-kill Studies. Having realized **CP-2** is a potent bactericidal agent with less toxicity than GS, we thereby envisioned whether its antibacterial mechanism resembles to those of typical AMPs, mainly consisting in the disruption of membrane. To prove it, we first conducted time-kill studies to investigate the bacteria killing kinetics of peptide **CP-2** and GS using *S. aureus* and *E. faecalis*. Both peptides can eradicate *S. aureus* very rapidly, as shown in **Figure 6A**. At a concentration of 25 or 50 μg/mL, **CP-2** can totally eliminate *S. aureus* in 4 h, in a similar way than GS although the kinetic was slightly slower for **CP-2**. Killing curves were also recorded on *E. faecalis* cells (**Figure 6B**). Again, **CP-2** and GS were very efficient for bacterial clearance since 2 hours were sufficient on *E. faecalis* cells with a slightly greater activity for **CP-2**. These data suggest that **CP-2** kills bacteria in a similar way than GS.

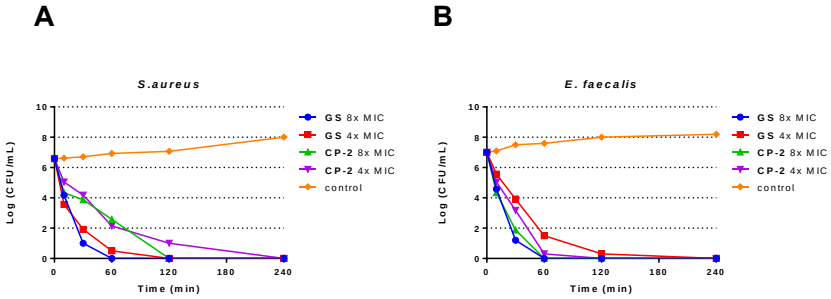

Figure 6. Time-kill curves of **CP-2** and GS for *S. aureus* (A) and *E. faecalis* (B). The killing activity was monitored for the first 4 h.

Cytoplasmic Membrane Depolarization. To elucidate whether the antibacterial mechanism of peptide **CP-2** involves the disruption of membrane, $DiSC_3$-5,[47] a membrane potential sensitive dye, was used to assess bacterial membrane depolarization on *S. aureus* and *E. faecalis*. When the cell membrane is intact, $DiSC_3$-5 is aggregates on the membrane and the fluorescence is self-quenched. However, upon membrane potential disruption, $DiSC_3$-5 is released and re-suspended in the buffer solution, leading to a fluorescence increase. Fluorescence was recorded over 30 minutes, as shown in **Figure 7**. On both assays, an immediate increase of fluorescence is observed upon the addition of **CP-2** (1x MIC) to the medium. A further increase was obtained by the addition of GS (1x MIC).These observations highlights that **CP-2** is capable to depolarize cytoplasmic membrane similar to GS.

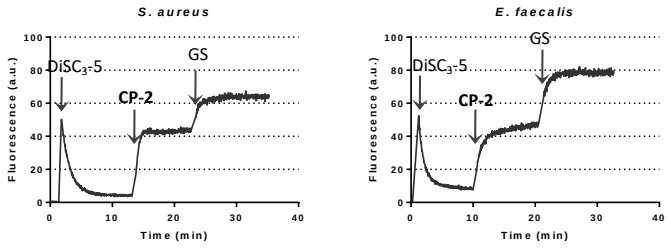

Figure 7. Cytoplasmic membrane depolarization of *S. aureus* (A) and *E. faecalis* (B) by peptide **CP-2** and GS.

Membrane Permeabilization. To further characterize the ability of **CP-2** to disrupt the membrane, we measured the membrane permeabilization using propidium iodide (PI). As it is well known, PI can go through impaired membranes and exhibit red fluorescence due to interactions with DNA.[48] **Figure 8** shows a time-course of fluorescence over 20 minutes. Upon the addition of peptides, an ever increasing fluorescence was recorded. On *S. aureus* cells, **CP-2** and GS (2x MIC) result in a similar fluorescence increase. Notably, **CP-2** has a stronger permeabilization effect than GS on *E. faecalis* cells at 2x MIC concentration.

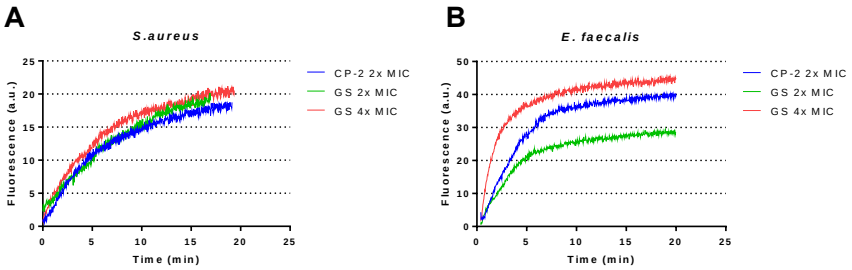

Figure 8. Membrane permeabilization of **CP-2** and GS. Enhancement of fluorescence was observed by uptake of membrane-impermeable PI upon addition of peptides to *S. aureus* (A) and *E. faecalis* (B).

Fluorescence Microscopy. Fluorescence microscopy experiments were also performed to assess the effect of our peptides on membrane permeabilization. As shown in **Figure 9**, the treatment by GS at 5x or 10x MIC concentration gave rise to a red fluorescence on both *S. aureus* and *E. faecalis* cells, suggesting that the membranes of these bacteria were disrupted. A similar phenomenon was observed when treated with peptide **CP-2**, albeit the intensity of fluorescence was less significant in comparison to GS at 10x MIC. These results further confirm that **CP-2** exhibits strong cytoplasmic membrane permeability.

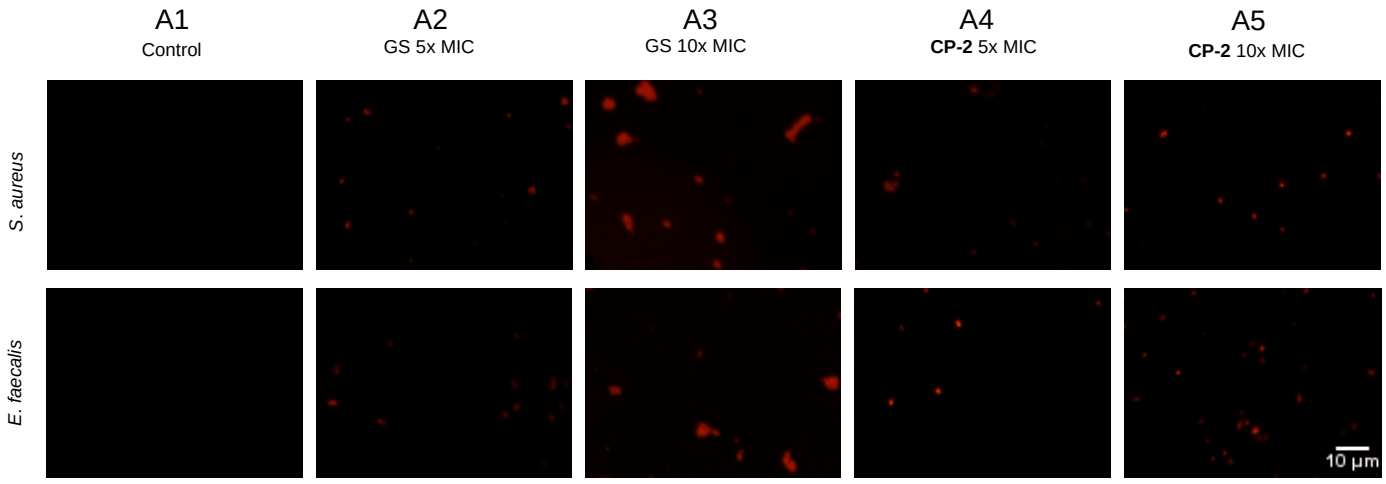

Figure 9. Fluorescence micrographs of *S.aureus* and *E. faecalis* that were treated with peptides for 1 h and PI stained. (A1) control, no treatment; (A2) treatment with GS at 5x MIC concentration; (A3) treatment with GS at 10x MIC concentration; (A4) treatment with **CP-2** at 5x MIC concentration; (A5) treatment with **CP-2** at 10x MIC concentration. Scale bar = 10 µm.

Scanning Electron Microscopy (SEM). Finally, SEM experiments were performed to visually examine the integrity of cell membranes upon exposure to **CP-2**. As shown in **Figure 10**, bacterial cells treated with 2x MIC concentration exhibited significant changes in their morphology compared to the intact cells. Briefly, the cell membrane of *S. aureus* was impaired to the point that cell contents leak out (arrows in **Figure 10**) when treated with 2x MIC concentration. Similarly, when treating with *E. faecalis* cells at 2x MIC, wrinkled cell walls were observed.

Taken together, both fluorescence (**Figure 7 to 9**) and SEM (**Figure 10**) experiments strongly indicate that the bactericidal mechanism of **CP-2** is associated with membrane disruption.

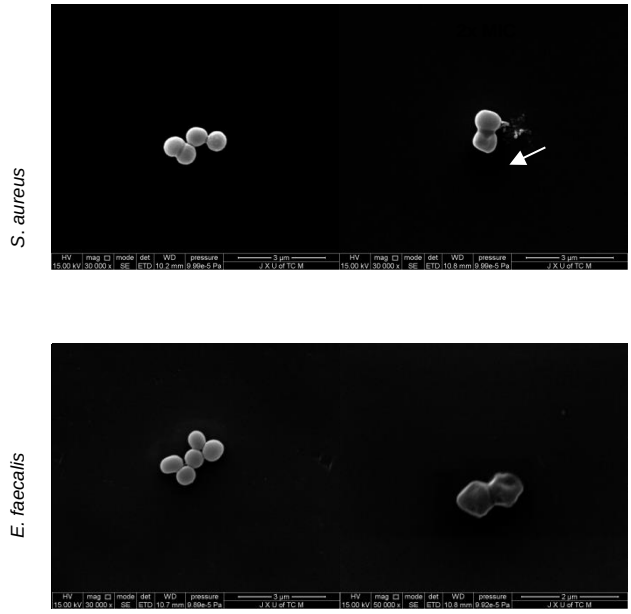

Figure 10. SEM photographs of **CP-2** treated and untreated bacteria (2x MIC concentration).

Conclusion

To conclude, a series of cyclopeptidomimetics inspired by the chemical skeleton of GS and incorporating β,γ-DiAA residues were synthesized and biologically evaluated. Within each β,γ-DiAA, two stereogenic carbon were used to create a chemical diversity in these new GS analogues family. Importantly, the β- and γ-carbons of the β,γ-DiAA motifs bear the NH2 and the benzyl groups, respectively. Their relative stereochemistry allows the control of the amphiphilic character required for the GS analogues activities. We have shown that with β*S* and γ*R*, **CP-2** is able to interact with SDS micelles and undergo folding in hydrophobic environments. In addition, among the tested antibacterial peptidomimetics, **CP-2** displays an antibacterial activity comparable to that of GS and exerts a lower toxicity towards human cells. Extensive mechanism studies suggested that **CP-2** kills bacteria through the disruption of cell membrane. This mode of action is the most promising for the development of new antibiotics since it is not subject to bacterial resistance. In future work, **CP-2** will be used as a structural framework for further chemical modifications in order to optimize the biological activities of this new class of bactericidal agents.

Experimental Section

General Remarks. Fmoc-amino acids and Fmoc-Pro-2-Chlorotrityl Chloride (CTC) Resin (1% cross-linked, 100-200 mesh, 0.476 mmol/g) were purchased from GL Biochem (Shanghai) Ltd. DMF was treated with CaH for overnight then distilled under reduce pressure. All other reagents and solvents were used directly without any further purification. Mass spectra were measured on a Microtof-Q Bruker Daltonics spectrometer coupled with a LC equipment (U3000 Thermofisher). Analytical RP-HPLC was performed on a Welch XB-C18 column (4.6 x 250 mm, 5 µm) running linear gradients CH_3CN (10-100%) into H_2O (0.1% TFA, v/v) over 60 min at 1 mL/min flow rate, with UV detection at 221 nm. Semi-preparative RP-HPLC purification was done on an YMC-Pack ODS-A (10x 250 mm, 5µm) running linear gradients of CH_3CN into H_2O (0.1% TFA, v/v) as indicated for each peptide, at a flow rate of 2 mL/min.

Synthesis. Synthesis of (β,γ)-DiAAs were described elsewhere.[42,49] Peptide synthesis was started from Fmoc-Pro-2-CTC–Resin by Automated Peptide Synthesis. During the sequential coupling, HBTU was used for activation, DiPEA as base, DMF as solvent and 20% piperidine for Fmoc deprotection. Resin cleavage was achieved in the condition of 1% TFA/DCM to keep the side-chain protecting groups intact. The subsequent macrocyclization was performed in diluted solution to minimize the hetero-condensation. After global deprotection under 90% TFA/H_2O (v/v), crude peptides were pre-purified by the precipitation in the presence of cold diethyl ether and then further purified by reverse phase high-performance liquid chromatography (RP-HPLC). After lyophilization, all peptides were prepared as white solid power.

Circular Dichroism Spectroscopy. CD spectra were recorded on a J-1500 CD Spectrometer (JASCO, Japan) using a circular quartz cell with a path length of 1 cm at 25 °C. Peptides were prepared at 0.1 mM aqueous solutions Spectra were recorded with a band width of 1 nm, a duration time of 1 s and a scan speed of 100 nm/min. Molar ellipticity is reported as mean residue ellipticity ($[\theta]_R$) in degrees.cm^2/dmol. Each measurement was repeated 3 times to calculate the mean value. The spectra from water were subtracted as background in data analysis.

Minimal Inhibitory Concentration Assay. MIC determination was performed according to our previously reported protocol.[42] Total seven bacteria covering both Gram-positive and Gram-negative strains were used in MIC determination: *Escherichia coli* (ATCC 25922), *Pseudomonas aeruginosa* (ATCC 27853), *Staphylococcus aureus* (ATCC 29213), *Bacillus subtilis* (ATCC 6633), *Streptococcus bovis* (ATCC 33317), *Enterococcus faecalis* (ATCC 29212) and *Enterococcus faecium* (ATCC 35667). Bacteria were inoculated for agar plate and incubated at Luria Bertani (LB) broth (*S. bovis* at Tryptic Soy Broth (TSB)) under constant shaking at 200 rpm for 4-6 h to mid-logarithmic phase and harvested by centrifugation (10000x g for 3 min). The bacterial cells were washed three times with PBS buffer (10 mM, pH 7.4), followed by resuspension to A_{620} 0.02 in LB or TSB broth. The samples were prepared as 1 mg/mL stock solution (2 mg/L solution for P. aeruginosa) in DMSO. The stock solution was double diluted to afford a series of 2-fold dilutions. Assays were performed on 96-well microtiter plates. Each microtiter well was filled with 10 μL (5 μL for P. aeruginosa) peptide solution in DMSO and 90 μL (95 μL for P. aeruginosa) suspension of a mid-logarithmic phase culture of bacteria. Cultures were carried out in triplicate. DMSO was used as negative control. The MICs were assessed by measuring turbidity at 620 nm after 48 h incubation at 37 °C. The 620 nm absorbance was measured on a Multiskan FC microplate reader (Thermo Scientific).

Bacterial Killing Kinetics. The kinetics of bacteria killing by the peptide **CP-2** and GS were tested. The bacteria *S. aureus* and *E. faecalis* were grown to mid-logarithmic phase in LB medium and harvested to make the suspension of 10^6 CFU/mL in PB medium. The suspension was incubated with peptide at 4x or 8x MIC concentration. The mixtures were diluted by 10^2 to 10^4 fold and spread on LB agar plates. After incubation at 37 °C for 24 h, the colonies on the plates were counted and plotted against the incubation time.

Hemolysis Assay. Hemolysis assay was reported elsewhere.[42] Human blood solution, 10% (w/v) SDS solution and PBS solution were freshly prepared. Peptides were dissolved in DMSO at 10 mg/mL as stock solution. The stock solution was diluted in DMSO to obtain a series of 2-fold dilutions. Fresh human blood solution was diluted to 5x10^5 erythrocytes per milliliter. For each well, 5 μL peptide, 45 μL PBS solution and 50 μL diluted blood solution was added. DMSO was used as negative control. SDS (0.1% w/v final concentration) was used as 100% hemolysis control. Cultures were carried out in triplicate and incubated for 30 min at 37 °C. Erythrocytes were separated by centrifugation (300 rpm, 10 min). A volume of 50 μL portion of each supernatant was transferred to a new 96 microtiter plate to measure the turbidity at 450 nm.

Cytotoxicity Assay. Peptides were dissolved in DMSO at 2.5 mg/mL as stock solution. The stock solution was diluted in cell medium (RPMI 1640, containing 100 U penicillin and 100 μg/mL streptomycin) supplemented with 1% fetal bovine serum to obtain a series of dilutions (0.1, 1, 5, 10 or 25 μg/mL). LO2 cells were applied in this work and were cultured in cell medium supplemented with 1% fetal bovine serum in a humidified incubator at 37 °C in 5% CO_2. The cells (5 x10^3 cells per well) were seeded in a 96-well plate in cell medium overnight. After culture medium removal, 100 μL medium containing different concentrations of peptide was added. Cultures were carried out in triplicate. After incubation for 24 h, the culture medium was removed, 100 μL fresh CCK-8 medium (90 μL cell medium and 10 μL CCK-8 solution) (Medchem Express, USA) was added to each well and the samples were incubated for another 2 h. The absorbance at 450 nm was measured by a SpectraMax i3x microplate reader (MD, USA).

Cytoplasmic Membrane Depolarization. *S.* aureus and *E. faecalis* were grown at LB broth under constant shaking at 200 rpm for 6 h to mid-logarithmic phase and harvested by centrifugation (10000x g for 3 min). The cells were washed three times with wash buffer (5 mM HEPES, 20 mM glucose, pH 7.4) and resuspended to A_{620} 0.05 (*S. aureus*) or 0.03 (*E. faecalis*) in the same buffer. Then, 0.1 M KCl was added to equilibrate the cytoplasmic and external K concentration. A volume of 2 mL of cell suspension was placed in a 1 cm cuvette followed by the addition of a $DiSC_3$-5 stock solution (4 mM in HEPES buffer) to a final concentration of 200 nM. The resulting solution was incubated until a stable reduction of fluorescence was achieved, indicating the successful uptake of the dye into the bacterial membrane. Changes in fluorescence were recorded with a CaryEclipse fluorescence spectrophotometer (Aginent, USA). After the addition of peptides (2x MIC), membrane depolarization was determined by monitoring the change in fluorescence emission intensity of the $DiSC_3$-5 dye at excitation and emission wavelengths of 622 and 670 nm, respectively. The addition of gramicidin S (4x MIC) was used to achieve maximum fluorescence.

Membrane Permeabilization. The bacteria *S. aureus* and *E. faecalis* were grown to mid-logarithmic phase in LB medium and harvested by centrifugation (10000x g for 3 min). The cells were washed three times with wash PBS buffer and resuspended to A_{620} 0.2 in the same buffer.

Then, the cell suspension was incubated with PI (5 μg/mL) for 15 min on ice in the dark. A volume of 2 mL of cell suspension was placed in a 1 cm cuvette followed by the addition of peptide at 2x or 4x MIC concentration. Membrane permeabilization was determined by monitoring the change in fluorescence emission intensity of the PI dye at excitation and emission wavelengths of 535 and 615 nm, respectively.

Fluorescence Microscopy. The bacteria *S. aureus* and *E. faecalis* were grown to mid-logarithmic phase in LB medium and harvested by centrifugation (10000x g for 3 min). The cells were washed three times with wash PBS buffer and resuspended to A_{620} 0.2 in the same buffer. Then, the cell suspension was incubated with peptide at 5x or 10x MIC concentration for 1 h. After centrifuged at 8000 rpm for 5 min, the cell pellets were washed with PBS buffer for three times, and incubated with PI (5 μg/mL) for 15 min on ice in the dark. The mixture was then centrifuged and the pellets were washed with the PBS buffer. Next, 10 μL of the samples were placed on chamber slides and observed under Eclipse Ni-U (Nikon, Japan).

Scanning Electron Microscopy. Bacteria were grown at LB broth under constant shaking at 200 rpm for 6 h to mid-logarithmic phase and harvested by centrifugation (10000x g for 3 min). The cells were washed three times with PBS buffer and resuspended to A_{620} 0.4 in the same medium. Peptide treatment of the bacterial cells was carried out at 37 °C for 1 h at their respective 2x MICs. Bacteria incubated with PBS served as the control. After the incubation, the cells were harvested by centrifugation (8000x g for 5min) and washed with PBS three times. Bacterial cells were then fixed with 2.5% (w/v) glutaraldehyde at 4 °C for 6 h. Before centrifugation at 8000x g for 3min, the cells were mixed by gently inverting the tube up and down for several minutes to prevent clumping of the cells. After three washes with PBS, the bacterial pellets were dehydrated for 15 min with a series of graded ethanol solutions (30, 50, 70, 80, 90 and 100%), the cells were mixed and centrifuged at 8000x g for 3 min. Following dehydration, the dried bacterial cells were transferred to dry alcohol. A volume of 10 uL of cell suspension was transferred to the cover slide and allowed to oven-dried at 60 °C for 5 min. The slides were coated and visualized under a scanning electron microscope (FEI Field Electron Microscope, Quanta 250, USA).

Acknowledgements

This work was financially supported by the National Natural Science Foundation of China (No. 21967012); State Key Laboratory for Chemistry and Molecular Engineering of Medicinal Resources (Guangxi Normal University, CMEMR2019-B07).

Keywords: peptidomimetics • antibiotics • membrane active • hemolysis • β,γ-diamino acids

[1] C. T. Walsh, T. A. Wencewicz, *J. Antibiot.* **2014**, *67*, 7–22.

[2] L. Czaplewski, R. Bax, M. Clokie, M. Dawson, H. Fairhead, V. A. Fischetti, S. Foster, B. F. Gilmore, R. E. W. Hancock, D. Harper, I. R. Henderson, K. Hilpert, B. V. Jones, A. Kadioglu, D. Knowles, S. Ólafsdóttir, D. Payne, S. Projan, S. Shaunak, J. Silverman, C. M. Thomas, T. J. Trust, P. Warn, J. H. Rex, *Lancet Infect. Dis.* **2016**, *16*, 239–251.

[3] J. Carlet, P. Collignon, D. Goldmann, H. Goossens, I. C. Gyssens, S. Harbarth, V. Jarlier, S. B. Levy, B. N'Doye, D. Pittet, R. Richtmann, W. H. Seto, J. W. van der Meer, A. Voss, *The Lancet* **2011**, *378*, 369–371.

[4] M. A. Cooper, D. Shlaes, *Nature* **2011**, *472*, 32–32.

[5] M. Mahlapuu, J. Håkansson, L. Ringstad, C. Björn, *Front. Cell. Infect. Microbiol.* **2016**, *6*, 194.

[6] G. Wang, X. Li, Z. Wang, *Nucleic Acids Res.* **2016**, *44*, D1087–D1093.

[7] M. Zasloff, *Nature* **2002**, *415*, 389–395.

[8] M. Wenzel, M. Rautenbach, J. A. Vosloo, T. Siersma, C. H. M. Aisenbrey, E. Zaitseva, W. E. Laubscher, W. van Rensburg, J. C. Behrends, B. Bechinger, L. W. Hamoen, *mBio* **2018**, *9*, e00802-18.

[9] J. D. Steckbeck, B. Deslouches, R. C. Montelaro, *Expert Opin Biol Ther* **2014**, *14*, 11–14.

[10] Q. Guan, S. Huang, Y. Jin, R. Campagne, V. Alezra, Y. Wan, *J. Med. Chem.* **2019**, *62*, 7603–7617.

[11] N. Dong, X. Zhu, S. Chou, A. Shan, W. Li, J. Jiang, *Biomaterials* **2014**, *35*, 8028–8039.

[12] F. Yuan, Y. Tian, W. Qin, J. Li, D. Yang, B. Zhao, F. Yin, Z. Li, *Org. Biomol. Chem.* **2018**, *16*, 5764–5770.

[13] S. Pal, U. Ghosh, R. S. Ampapathi, T. K. Chakraborty, in *Peptidomimetics II* (Ed.: W. Lubell), Springer International Publishing, Cham, **2015**, pp. 159–202.

[14] R. Nordström, M. Malmsten, *Adv. Colloid Interface Sci.* **2017**, *242*, 17–34.

[15] F. I. Nollmann, T. Goldbach, N. Berthold, R. Hoffmann, *Angew. Chem. Int. Ed.* **2013**, *52*, 7597–7599.

[16] R. Nordström, L. Nyström, H. Ilyas, H. S. Atreya, B. C. Borro, A. Bhunia, M. Malmsten, *Colloids Surf., A* **2019**, *565*, 8–15.

[17] Y. Gong, D. Andina, S. Nahar, J.-C. Leroux, M. A. Gauthier, *Chem. Sci.* **2017**, *8*, 4082–4086.

[18] O. Babii, S. Afonin, A. Yu. Ishchenko, T. Schober, A. O. Negelia, G. M. Tolstanova, L. V. Garmanchuk, L. I. Ostapchenko, I. V. Komarov, A. S. Ulrich, *J. Med. Chem.* **2018**, *61*, 10793–10813.

[19] O. Babii, S. Afonin, M. Berditsch, S. Reisser, P. K. Mykhailiuk, V. S. Kubyshkin, T. Steinbrecher, A. S. Ulrich, I. V. Komarov, *Angew. Chem. Int. Ed.* **2014**, *53*, 3392–3395.

[20] Y. Q. Yeoh, J. Yu, S. W. Polyak, J. R. Horsley, A. D. Abell, *ChemBioChem* **2018**, *19*, 2591–2597.

[21] P. Claudon, A. Violette, K. Lamour, M. Decossas, S. Fournel, B. Heurtault, J. Godet, Y. Mély, B. Jamart-Grégoire, M.-C. Averlant-Petit, J.-P. Briand, G. Duportail, H. Monteil, G. Guichard, *Angew. Chem. Int. Ed.* **2010**, *49*, 333–336.

[22] P. Li, C. Zhou, S. Rayatpisheh, K. Ye, Y. F. Poon, P. T. Hammond, H. Duan, M. B. Chan-Park, *Adv. Mater.* **2012**, *24*, 4130–4137.

[23] M. Zhu, P. Liu, H. Shi, Y. Tian, X. Ju, S. Jiang, Z. Li, M. Wu, Z. Niu, *J. Mater. Chem. B* **2018**, *6*, 3884–3893.

[24] M. Bagheri, M. Amininasab, M. Dathe, *Chem. Eur. J.* **2018**, *24*, 14242–14253.

[25] M.-R. Lee, N. Raman, S. H. Gellman, D. M. Lynn, S. P. Palecek, *ACS Chem. Biol.* **2017**, *12*, 2975–2980.

[26] R. Shyam, N. Charbonnel, A. Job, C. Blavignac, C. Forestier, C. Taillefumier, S. Faure, *ChemMedChem* **2018**, *13*, 1513–1516.

[27] Kuppusamy, Willcox, Black, Kumar, *Antibiotics* **2019**, *8*, 44.

[28] H. Yamamura, K. Isshiki, Y. Fujita, H. Kato, T. Katsu, K. Masuda, K. Osawa, A. Miyagawa, *Med. Chem. Commun.* **2019**, *10*, 1432–1437.

[29] L. H. Kondejewski, S. W. Farmer, D. S. Wishart, R. E. w. Hancock, R. S. Hodges, *Int. J. Pept. Protein Res.* **1996**, *47*, 460–466.

[30] M. Berditsch, S. Afonin, J. Reuster, H. Lux, K. Schkolin, O. Babii, D. S. Radchenko, I. Abdullah, N. William, V. Middel, U. Strähle, A. Nelson, K. Valko, A. S. Ulrich, *Sci Rep* **2019**, *9*, 17938.

[31] O. Babii, S. Afonin, L. V. Garmanchuk, V. V. Nikulina, T. V. Nikolaienko, O. V. Storozhuk, D. V. Shelest, O. I. Dasyukevich, L. I. Ostapchenko, V. Iurchenko, S. Zozulya, A. S. Ulrich, I. V. Komarov, *Angew. Chem. Int. Ed.* **2016**, *55*, 5493–5496.

[32] A. L. Llamas-Saiz, G. M. Grotenbreg, M. Overhand, M. J. van Raaij, *Acta Crystallogr. D Biol. Crystallogr* **2007**, *63*, 401–407.

[33] A. Asano, M. Doi, *X-Ray Struct. Anal. Online* **2019**, *35*, 1–2.

[34] L. H. Kondejewski, S. W. Farmer, D. S. Wishart, C. M. Kay, R. E. W. Hancock, R. S. Hodges, *J. Biol. Chem.* **1996**, *271*, 25261–25268.

[35] G. M. Grotenbreg, A. E. M. Buizert, A. L. Llamas-Saiz, E. Spalburg, P. A. V. van Hooft, A. J. de Neeling, D. Noort, M. J. van Raaij, G. A. van der Marel, H. S. Overkleeft, M. Overhand, *J. Am. Chem. Soc.* **2006**, *128*, 7559–7565.

[36] M. Tamaki, I. Sasaki, M. Kokuno, M. Shindo, M. Kimura, Y. Uchida, *Org. Biomol. Chem.* **2010**, *8*, 1791.

[37] C. Solanas, B. G. de la Torre, M. Fernández-Reyes, C. M. Santiveri, M. Á. Jiménez, L. Rivas, A. I. Jiménez, D. Andreu, C. Cativiela, *J. Med. Chem.* **2009**, *52*, 664–674.

[38] F. Bouillère, D. Feytens, D. Gori, R. Guillot, C. Kouklovsky, E. Miclet, V. Alezra, *Chem. Commun.* **2012**, *48*, 1982–1984.

[39] S. Thétiot-Laurent, F. Bouillère, J.-P. Baltaze, F. Brisset, D. Feytens, C. Kouklovsky, E. Miclet, V. Alezra, *Org. Biomol. Chem.* **2012**, *10*, 9660–9663.

[40] A. Stanovych, R. Guillot, C. Kouklovsky, E. Miclet, V. Alezra, *Amino Acids* **2014**, *46*, 2753–2757.

[41] Y. Wan, N. Auberger, S. Thétiot-Laurent, F. Bouillère, A. Zulauf, J. He, S. Courtiol-Legourd, R. Guillot, C. Kouklovsky, S. Cote des Combes, C. Pacaud, I. Devillers, V. Alezra, *Eur. J. Org. Chem.* **2018**, *2018*, 329–340.

[42] Y. Wan, A. Stanovych, D. Gori, S. Zirah, C. Kouklovsky, V. Alezra, *Eur. J. Med. Chem.* **2018**, *149*, 122–128.

[43] Q. Guan, K. Chen, Q. Chen, J. Hu, K. Cheng, C. Hu, J. Zhu, Y. Jin, E. Miclet, V. Alezra, Y. Wan, *ChemMedChem* **2020**, *15*, 1089–1100.

[44] Y. Wan, J.-P. Baltaze, C. Kouklovsky, E. Miclet, V. Alezra, *J. Pept. Sci.* **2019**, *25*, e3143.

[45] N. Auberger, A. Stanovych, S. Thétiot-Laurent, R. Guillot, C. Kouklovsky, S. C. des Combes, C. Pacaud, I. Devillers, V. Alezra, *Amino Acids* **2016**, *48*, 2237–2242.

[46] A. C. Gibbs, L. H. Kondejewski, W. Gronwald, A. M. Nip, R. S. Hodges, B. D. Sykes, D. S. Wishart, *Nature Structural Biology* **1998**, *5*, 284–288.

[47] L. Zhang, P. Dhillon, H. Yan, S. Farmer, R. E. W. Hancock, *Antimicrob. Agents Chemother.* **2000**, *44*, 3317–3321.

[48] M. Wenzel, M. Patra, C. H. R. Senges, I. Ott, J. J. Stepanek, A. Pinto, P. Prochnow, C. Vuong, S. Langklotz, N. Metzler-Nolte, J. E. Bandow, *ACS Chem. Biol.* **2013**, *8*, 1442–1450.

[49] C. T. Hoang, F. Bouillère, S. Johannesen, A. Zulauf, C. Panel, A. Pouilhès, D. Gori, V. Alezra, C. Kouklovsky, *J. Org. Chem.* **2009**, *74*, 4177–4187.